ACS OMEGA

Open Access

http://pubs.acs.org/journal/acsodf

Article

Efficient Isolation and Enrichment of SH2 Domain Protein Species from Plasma Exploiting Specific Peptide−Protein Interactions

Zhen-Cun Cai, Long-Long Zhao, Qing Chen,* and Xue Hu*

Cite This: *ACS Omega* 2025, 10, 55316−55324

Read Online

ACCESS | Metrics & More | Article Recommendations | Supporting Information

ABSTRACT: Fiber SiO_2 microspheres are modified with a phosphorylated peptide chain through a Schiff base reaction, and the product, pPeps@SiO_2 microspheres, is obtained. The interaction between the phosphorylated peptide chain and the specific site of the SH2 domain offers the as-prepared microspheres with good capture performance toward SH2 domain proteins. Under the condition of pH 4, the capture efficiencies of pPeps@SiO_2 microspheres for SH2-containing proteins SH2−SH2, SH2−SH3, and SH2−PTP are 91%, 61.3%, and 62.96%, respectively, which are much higher than those for proteins without an SH2 domain. The adsorbed SH2 proteins can be readily recovered by using 0.1 mol L^{-1} imidazole; therefore, a strategy for the isolation of SH2 domain proteins from complex matrices is proposed. SDS-PAGE results indicate that the isolation of the SH2−SH3 protein from plasma using pPeps@SiO_2 microspheres is successfully achieved, and the isolation process is not affected by other high-abundance protein species in plasma. The concentration of SH2 domain protein in plasma increases from 12.4 pg mL^{-1} to 61.59 pg mL^{-1} after treating with pPeps@SiO_2 microspheres, which well demonstrates the favorable separation and enrichment ability of pPeps@SiO_2 microspheres. The isolation strategy based on protein domains not only provides the basis for in-depth investigation of SH2 domain protein functions but also provides new ideas for protein separation and purification.

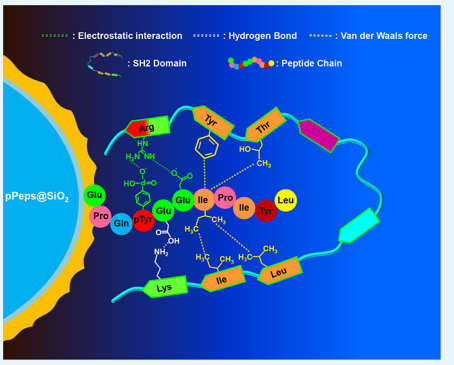

INTRODUCTION

Protein interactions are a complicated issue in proteomic research, and the protein domain is the starting point for studying protein interaction.[1] The Src homology 2 (SH2) domain, a protein module comprising approximately 100 amino acids, was first identified in the oncogenic protein v-Src[2] and subsequently found in hundreds of human protein species.[3] All the known SH2 domains are conservative folded and include an antiparallel β-sheet in the middle and a sandwich-like structure of α-helices on each side.[4−9] The SH2 domain can specifically recognize phosphorylated tyrosine (pTyr) and 3−6 amino acid residues at the C-terminus of pTyr,[10−14] and it is an important part of the tyrosine kinase signal transduction pathway. The activation of cancer genes such as Src, Abl, Ras, and Raf, due to the enhancement of tyrosine kinase activity, is directly or indirectly mediated by the SH2 domain.[15] The abnormality of the signaling pathway involving the SH2 domain is related to a variety of tumors and genetic diseases.[16] In patients with chronic myelogenous leukemia, it was found that the SH2 domain with a self-inhibition function upstream of Abl is missing, which leads to increased kinase activity. The target molecules Shc and p62, recruited by the hyperphosphorylated SH2 domain, indirectly enhance the Ras pathway.[17] Previous research has indicated that various growth factor receptors play significant roles in the initiation and progression of diverse tumor types. Grb2 is the main pathway of growth factor receptor-mediated signal transmission, so its SH2 domain target molecular mimics are expected to block the conduction of this signaling pathway.[18] Abnormalities in the SH2 domain have also been found in some genetic diseases. Point mutations or deletion mutations in the SH2 domain of the SAP protein will cause X-linked lymphocytosis.[19] A single-point mutation within the SH2 domain of Bruton's tyrosine kinase has been implicated in the onset of X-linked agammaglobulinemia.[20] Similarly, mutations in the kinase domain of ZAP-70 may result in severe combined immunodeficiency (SCID).[21] Noonan syndrome patients have point mutations in the *N*-terminal gene encoding the SH2 domain of the SHP-2 molecule.[22] STAT5b, expressed by patients with growth hormone insensitivity syndrome, contains only half of the SH2 domain and so on.[23]

Considering the extensive existence of the SH2 domain in different protein species and its role in regulating corresponding signal transduction pathways,[24] the investigation on the SH2 domain's ligand recognition characteristics and the corresponding target molecular mimics is quite favored by

Received: May 1, 2025
Revised: September 29, 2025
Accepted: November 5, 2025
Published: November 12, 2025

Scheme 1. Schematic Illustration of the Preparation Process for pPeps@SiO_2 Microspheres

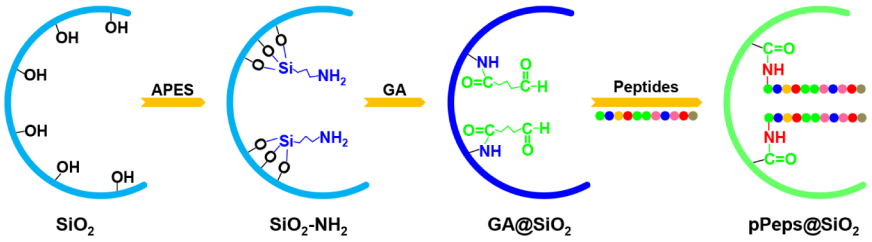

biologists and pharmacists. Cantley and colleagues demonstrated that the SH2 domain selectively recognizes phosphotyrosine-containing proteins or synthetic peptides based on specific amino acid sequences, while showing minimal affinity for their unphosphorylated counterparts.[25] Fantl et al. reported that peptides containing the pTyr-Met/Val-X-Met sequence exhibit high affinity for phosphatidylinositol 3-kinase, while the replacement of the Met residue at the end of the sequence induces a significant reduction in affinity.[26] Peptides containing the sequence Tyr-X-X-Leu/Ile (about 10 amino acids) can specifically recognize the SH2 domain contained in the Src family,[27] and a bidentate-binding mode is formed between this amino acid sequence and tyrosine kinases with two SH2 domains.[28] Several strategies have been previously developed for SH2 domain protein isolation using synthetic phosphorylated peptides. For instance, Testini et al. employed phosphopeptide-based affinity resins to investigate VEGFR2 signaling via SH2 interactions, while Höfener et al. utilized Inhibitor Affinity Purification (IAP) to probe SH2-domain interactions in proteomic workflows.[29,30] Building upon these foundational studies, we designed a novel platform by grafting phosphotyrosine-containing peptides onto fibrous SiO_2 microspheres, which offer higher surface area and better accessibility compared to conventional supports. This design enables the selective enrichment of SH2-domain proteins through noncovalent interactions, forming the basis of our separation strategy.

Generally, materials with a pore structure are collectively referred to as porous materials. Based on pore size, pore structures are typically classified into three categories: macropores (>50 nm), mesopores (2−50 nm), and micropores (<2 nm). Studies have shown that the penetrating mesoporous and macroporous structures are beneficial for reducing diffusion resistance, providing a larger contact area, and offering more active sites.[31−33] Silica-based porous substances have gained widespread attention due to their excellent resistance to acidic and basic environments, ease of synthesis through various techniques, and abundant raw material sources. In particular, fibrous silica microspheres possess a broadly distributed mesoporous network, and their fiber-like architecture can also function as a macroporous framework, endowing them with a hierarchical porous structure.[34−38] Therefore, this work selects fibrous SiO_2 microspheres as the carrier to carry the polypeptide chain to achieve the separation and purification of proteins.

The binding of the SH2 domain to tyrosine-phosphorylated proteins or peptide chains primarily depends on the amino acid sequence surrounding the phosphotyrosine residue, and the arrangement of amino acids around phosphorylated tyrosine is the key to achieving specific binding. Therefore, we delicately designed phosphorylated tyrosine-containing peptide chains with specific amino acid arrangements and immobilized them on porous fibrous SiO_2 nanoparticles via Schiff base reactions to achieve the separation and enrichment of SH2 domain proteins from complex samples, i.e., human plasma.

EXPERIMENTAL SECTION

Materials and Reagents. See details in Supporting Information.

Instruments. See details in the Supporting Information.

Fabrication of pPeps@SiO_2 Microspheres. The fibrous SiO_2 microspheres were sequentially modified to obtain the final peptide-functionalized materials. First, SiO_2−NH_2 microspheres were prepared by reacting pristine fibrous SiO_2 with (3-aminopropyl)triethoxysilane (APTES), introducing surface amino groups. These amino-functionalized microspheres were then treated with 2.5% glutaraldehyde (GA) to obtain GA@SiO_2 microspheres via Schiff base activation. Finally, phosphorylated peptides (pPep1) were covalently immobilized onto GA@SiO_2 through the reaction with terminal amine groups, forming the final pPeps@SiO_2 microspheres. These modified microspheres were thoroughly washed with PBS and stored at 4 °C prior to use. Detailed synthesis protocols for each modification step are provided in the Supporting Information.

Adsorption of Proteins by pPeps@SiO_2 Microspheres. To evaluate the protein adsorption capacity of pPeps@SiO_2 microspheres, a range of protein models, including SH2−SH2, SH2−SH3, SH2−PTP, PTP, HSA, IgG, and Trf, are employed. In the typical procedure, 1 mL of the protein solution is incubated with 2 mg of the microspheres at ambient temperature under vigorous shaking for 30 min to facilitate binding. Following incubation, the suspension is subjected to centrifugation at 6000 rpm for 5 min. The resulting supernatant is analyzed for unbound protein content via absorbance measurement at 595 nm, following the Bradford method. The quantity of adsorbed protein (Q) is subsequently determined using the corresponding formula:

$$Q = \frac{(C_0 - C_1) \times V}{M}$$

where C_0 and C_1 represent the initial and residual protein concentrations ($mg \cdot L^{-1}$), V denotes the volume of the protein solution (L), and M refers to the mass of the adsorbent (g).

The pPeps@SiO_2 microspheres with adsorbed proteins are then washed with deionized water and incubated with 1 mL of 0.1 $mol \cdot L^{-1}$ imidazole solution. After shaking for 30 min, the mixture is centrifuged at 6000 rpm for 5 min, and the supernatant is collected for subsequent SDS-PAGE analysis and quantitative assays.

RESULTS AND DISCUSSION

Preparation and Characterization of pPeps@SiO_2 Microspheres. The preparation of pPeps@SiO_2 microspheres

https://doi.org/10.1021/acsomega.5c04034
ACS Omega 2025, 10, 55316−55324

involves four steps, as illustrated in Scheme 1. pPeps@SiO_2 microspheres are first synthesized according to a hydrothermal synthesis procedure[39] and then modified with amino propyltriethoxysilane. The phosphorylated peptide pPep1 (sequence: Glu-Pro-Gln-pTyr-Glu-Glu-Ile-Pro-Ile-Tyr-Leu), containing a central phosphotyrosine residue, was designed based on canonical SH2-binding motifs, especially those recognized by Src-family kinase SH2 domains.[40] Such sequences typically contain a central phosphotyrosine (pTyr) flanked by acidic or hydrophobic residues at the +1 to +3 positions, which are known to enhance specificity and affinity. To better contextualize the design of our phosphorylated peptide (pPep1), we compiled a comparison table (Table 1)

Table 1. Comparison of Representative SH2 Domain-Binding Peptide Sequences

Peptide Name	Sequence (N→C)
pYVNV[12]	pTyr-Val-Asn-Val
Crk-SH2 canonical motif[13]	Glu-pTyr-Val-Asn
pYEEI[25]	pTyr-Glu-Glu-Ile
VEGFR2-SH2 binding[29]	Gln-pTyr-Leu-Asn
Inhibitor affinity probe[30]	Ac-pTyr-Ala-Pro-Leu
GpYLPQTV[41]	Gly-pTyr-Leu-Pro-Gln-Thr-Val
pYENV[42]	pTyr-Glu-Asn-Val
pPep1 (this work)	Glu-Pro-Gln-pTyr-Glu-Glu-Ile-Pro-Ile-Tyr-Leu

summarizing representative SH2-binding sequences previously reported in the literature. These canonical motifs generally feature a central phosphotyrosine flanked by residues that modulate domain-specific binding. In contrast, pPep1 was rationally designed to enhance both SH2-domain affinity and compatibility with immobilization onto fibrous SiO_2 surfaces. The inclusion of multiple Glu and hydrophobic residues at the +1 to +5 positions provides enhanced electrostatic and hydrophobic interaction potential, distinguishing it from shorter or naturally occurring SH2-binding sequences. This peptide was covalently attached to the surface of fibrous SiO_2 microspheres through a Schiff base reaction, which occurs between the aldehyde groups of glutaraldehyde and the amino groups of the peptides, resulting in the formation of pPeps@SiO_2 microspheres. To confirm the phosphorylation-dependent binding specificity of the SH2 domain, a solution-phase binding assay was performed using the nonphosphorylated control peptide pPep2 (sequence: Glu-Pro-Gln-Tyr-Glu-Glu-Ile-Pro-Ile-Tyr-Leu). Given that SH2 domains are known to specifically recognize phosphotyrosine-containing motifs, the absence of detectable interactions with pPep2 served as a negative control, reinforcing the critical role of phosphorylation in mediating the observed binding. Accordingly, pPep2 was not immobilized on the microspheres and was exclusively employed in the solution-phase experiments.

The SEM reveals that the fibrous SiO_2 microspheres exhibit a spherical morphology composed of intertwined fibers, with an average diameter of approximately 500 nm, and display a typical mesoporous architecture (Figure 1A). Following modification with polypeptide chains, the mesoporous features of the microspheres are well preserved (Figure 1B). As shown in Figure 1D, the TEM image of the pPeps@SiO_2 microspheres reveals an increase in particle size and a decrease in pore diameter compared to that of the unmodified fibrous SiO_2 microspheres (Figure 1C). The EDX mapping images of

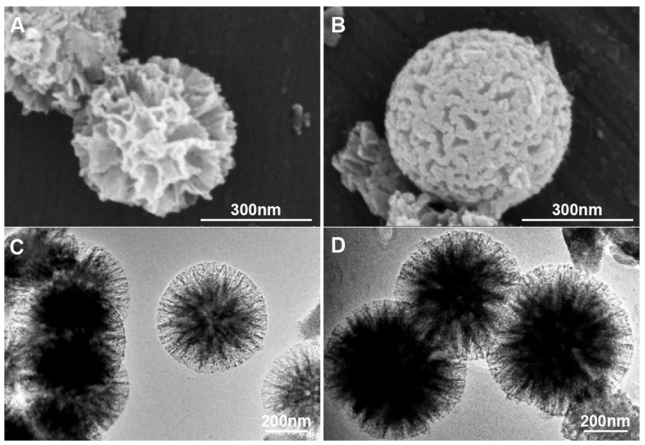

Figure 1. SEM images of fibrous SiO_2 microspheres (A) and pPeps@SiO_2 microspheres (B). TEM images of fibrous SiO_2 microspheres (C) and pPeps@SiO_2 microspheres (D).

pPeps@SiO_2 microspheres reveal the successful formation of the fibrous SiO_2 framework. C, N, and P are uniformly distributed across the surface, and the contents were 12%, 6%, and 23%, respectively (Figure 2). These values represent the relative atomic percentages of each element detected on the microsphere surface, rather than the bulk composition. The relatively high phosphorus content arises from localized enrichment of phosphate groups introduced by the phosphotyrosine peptides.[43] As EDX is surface-sensitive and detects elements within the top 1−2 μm of the sample, the observed phosphorus level reflects successful and dense peptide grafting rather than overall microsphere composition.[44,45] This shows that the polypeptide chain is successfully modified onto the surface of the fibrous SiO_2 microspheres and is homogeneously distributed.

X-ray photoelectron spectroscopy (XPS) was utilized to investigate the chemical states of N and C elements in SiO_2−NH_2 microspheres, GA@SiO_2 microspheres, and pPeps@SiO_2 microspheres (Figure 3). The N 1s spectrum shown in Figure 3A, compared with SiO_2−NH_2, shows that both GA@SiO_2 microspheres and pPeps@SiO_2 microspheres have O═C−NH (401.3 eV) except $-NH_2$ (399.6 eV), and GA@SiO_2 microspheres also have −NH− (400.4 eV), which is attributed to peptide chain side chain functional groups. The C 1s spectra (Figure 3B) of SiO_2−NH_2 were fitted into C−C (284.6 eV) and −C−N (285.3 eV).[46] Compared with SiO_2−NH_2, both GA@SiO_2 microspheres and pPeps@SiO_2 microspheres have O═C−NH (285.9 eV) and C−O (286.4 eV). Compared with GA@SiO_2, SiO_2@pPeps shows a significant increase in the N 1s peak of O═C−NH after modifying the polypeptide chain. This further proves that the polypeptide chain was effectively grafted onto the microsphere surface.

The BET analysis reveals that the specific surface areas and total pore volumes of fibrous SiO_2, GA@SiO_2, and pPeps@SiO_2 microspheres are approximately 569.36 $m^2 \cdot g^{-1}$ and 2.111 $cm^3 \cdot g^{-1}$, 228.39 $m^2 \cdot g^{-1}$ and 1.365 $cm^3 \cdot g^{-1}$, and 148.65 $m^2 \cdot g^{-1}$ and 1.150 $cm^3 \cdot g^{-1}$, respectively. Nitrogen adsorption−desorption isotherms of pPeps@SiO_2 microspheres exhibit a typical type IV pattern with an H3 hysteresis loop (Figure 4A), confirming that the mesoporous architecture is retained following functionalization with polypeptide chains. FT-IR spectra of fibrous SiO_2 microspheres, GA@SiO_2 microspheres, and pPeps@SiO_2 microspheres are illustrated in Figure 4B.

https://doi.org/10.1021/acsomega.5c04034
ACS Omega 2025, 10, 55316−55324

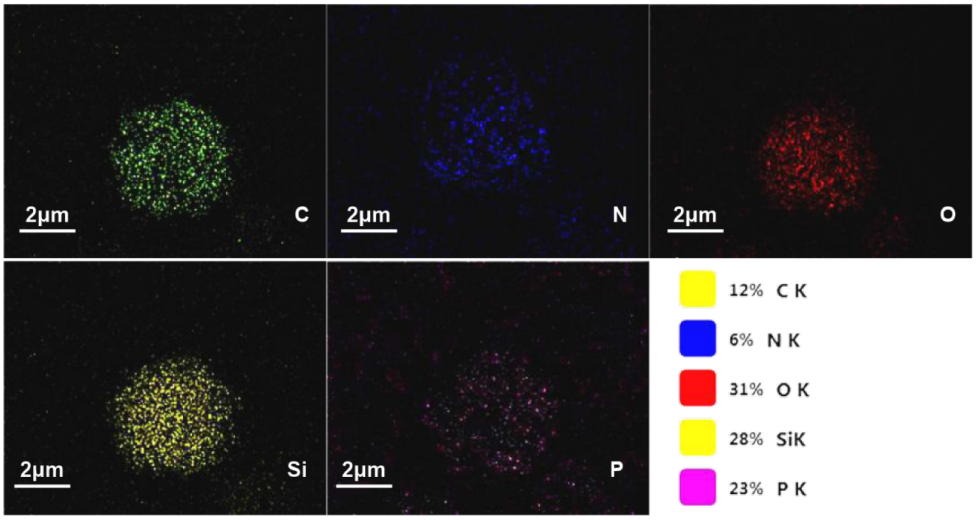

Figure 2. EDX mapping images of pPeps@SiO_2 microspheres.

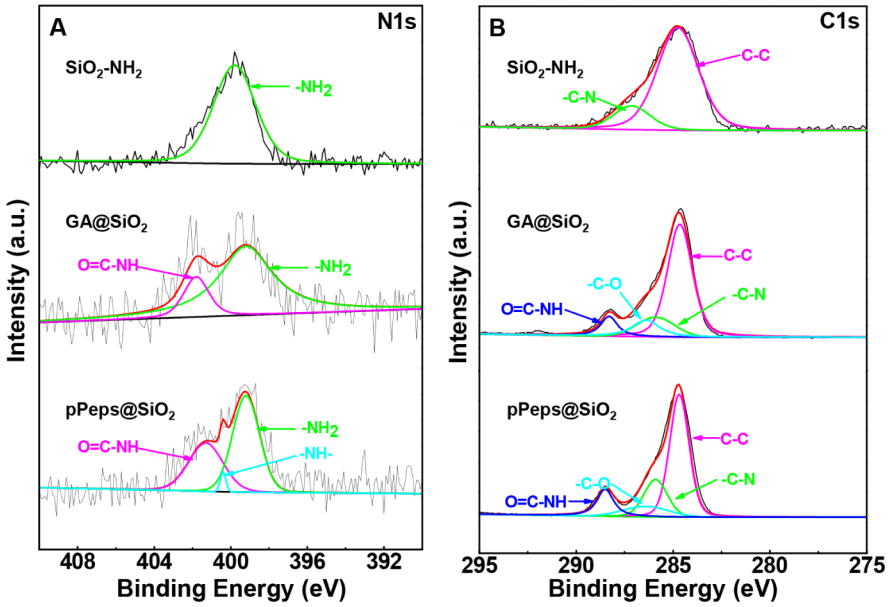

Figure 3. XPS analysis of (A) high-resolution C 1s spectrum and (B) high-resolution N 1s spectrum of SiO_2−NH_2 microspheres, GA@SiO_2 microspheres, and pPeps@SiO_2 microspheres.

The GA@SiO_2 and pPeps@SiO_2 microspheres display characteristic absorption peaks at 2957 cm^{-1} and 2856 cm^{-1}, corresponding to the asymmetric bending vibrations of $-CH_3$ and $-CH_2$ groups, respectively.[47] The absorption peaks of pPeps@SiO_2 microspheres at 1635 cm^{-1}, 1460 cm^{-1}, and 3437 cm^{-1} are attributed to the trans and cis structures of peptide bond stretching vibrations of −NH−. These above characteristic peaks suggest the functionalization of polypeptide chains on the final pPeps@SiO_2 microspheres through polypeptide chain modification.

The broad diffraction peak observed at 2θ = 22.13° in the XRD patterns of both fibrous SiO_2 microspheres and pPeps@SiO_2 microspheres indicates that the structural integrity of the SiO_2 framework remains unaffected by polypeptide chain modification (Figure 4C). TGA results indicate that fibrous SiO_2, aminated SiO_2 (SiO_2−NH_2), GA@SiO_2, and pPeps@SiO_2 microspheres all exhibit an initial weight loss around 100 °C, which is attributed to the release of physically adsorbed or crystalline water (Figure 4D). It can be seen from the curve that the organic layer on the surface of the fibrous SiO_2 microspheres begins to decompose at about 200 °C. From the DTG curve of pPeps@SiO_2 microspheres (Figure S1), it can be seen that the material has an endothermic peak at about 210 °C, which corresponds to the decomposition of the amino group on the surface of the microspheres, and there is an endothermic peak around 461 °C, which represents the decomposition peak of the modified polypeptide chain.

Binding Ability of Phosphotyrosine-Containing Peptides to SH2 Domain Protein. While biophysical techniques, such as isothermal titration calorimetry (ITC), fluorescence polarization (FP), or gel mobility shift assays, are widely used to characterize protein−ligand interactions with quantitative affinity data, the current study focuses on confirming the structural composition and stoichiometry of peptide−protein complexes. ESI-MS, though indirect in determining binding strength, provides a powerful and

https://doi.org/10.1021/acsomega.5c04034
ACS Omega 2025, 10, 55316−55324

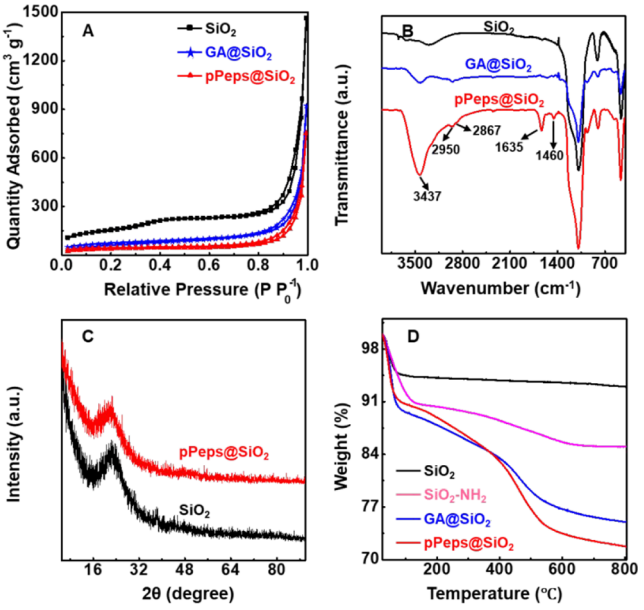

Figure 4. Nitrogen adsorption−desorption isotherms of fibrous SiO_2, GA@SiO_2, and pPeps@SiO_2 microspheres (A). FT-IR spectra of fibrous SiO_2, GA@SiO_2, and pPeps@SiO_2 microspheres (B). XRD patterns of fibrous SiO_2 and pPeps@SiO_2 microspheres (C). TGA curves of fibrous SiO_2, SiO_2−NH_2, GA@SiO_2, and pPeps@SiO_2 microspheres (D).

sensitive means to directly detect noncovalent complexes under mild conditions. In particular, it is well suited for verifying the successful formation of specific peptide−SH2 domain interactions, especially in combination with functional enrichment assays. Therefore, the use of ESI-MS in this context is both appropriate and effective for the intended analytical purpose. Figure 5 shows the ESI mass spectra of the SH2 domain protein SH2−SH3 and the binding of SH2−SH3 to different ratios of specifically designed peptide chains. The molecular weight of SH2−SH3 protein was confirmed by electrospray ionization mass spectrometry (ESI-MS). As shown in Figure 5A, SH2−SH3 displayed a typical multiply charged pattern with characteristic m/z peaks at 820.02, 851.55, 885.56, 922.43, 962.49, 1006.15, 1054.08, 1106.76, and 1164.99. Among these, the peak at m/z = 1164.99 with a charge state of z = 19+ corresponds to a calculated molecular mass of 22,114.6 Da, which closely matches the theoretical molecular weight of SH2−SH3 (∼22.2 kDa).[48,49] This strongly supports the correct identification and integrity of the protein under native ESI-MS conditions. It can be seen from Figure 5B that a small amount of free SH2−SH3 exists when the ratio of SH2−SH3 to the phosphorylated tyrosine peptide chain is 1:1, but when the ratio increases to 1:10 (Figure 5C), the signal of free SH2−SH3 cannot be observed, indicating that SH2−SH3 has been completely combined with the peptide chain to form a noncovalent complex. To elucidate the mass shift upon peptide binding, we focus on the peak at m/z = 840.50 in Figure 5B, which corresponds to the [M + 28H]^28+ ion of the SH2−SH3−pPep1 complex. This peak reflects the addition of the peptide mass (approximately 1,554.6 Da) to the SH2−SH3 domain (22,114.6 Da), resulting in a complex with a total mass of 23,668.85 Da. The observed m/z shift from the unbound SH2−SH3 at $m/z \approx$ 814.13 to the complex at m/z = 840.50 confirms the binding of pPep1, as the mass difference is consistent with the peptide's mass distributed over the 28 positive charges.[50,51] While for the nonphosphotyrosine peptide chain, even when the concentration is increased to 10 times that of SH2−SH3, the formation of complexes is still not observed (Figure 5D). These results strongly suggest the binding specificity of the SH2 domain protein toward the phosphorylated tyrosine peptide.

Protein-Capturing Behaviors by pPeps@SiO_2 Microspheres. The capturing behaviors of SH2−SH2, SH2−SH3, SH2−PTP, PTP, HSA, IgG, and Trf onto pPeps@SiO_2 microspheres were examined across a range of pH conditions. As illustrated in Figure 6A, SH2 domain-containing proteins exhibit significantly higher adsorption compared to non-SH2 proteins under pH 4.0 conditions. The adsorption efficiencies for SH2−SH2, SH2−SH3, and SH2−PTP at pH 4.0 are 91%,

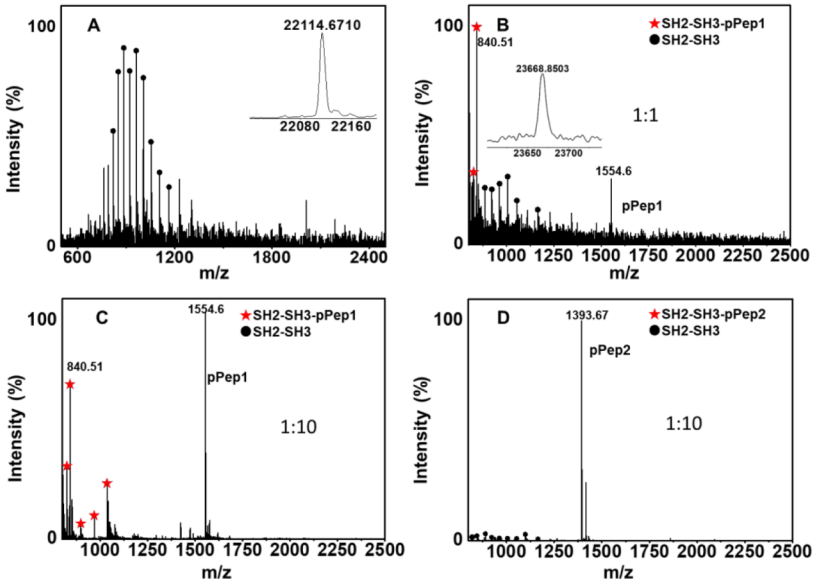

Figure 5. Electrospray ionization mass spectra of SH2−SH3 (A), 1:1 SH2−SH3 protein:pPep1 molar ratio (B), 1:10 ratio with pPep1 (C), and 1:10 ratio with pPep2 (D).

https://doi.org/10.1021/acsomega.5c04034
ACS Omega 2025, 10, 55316−55324

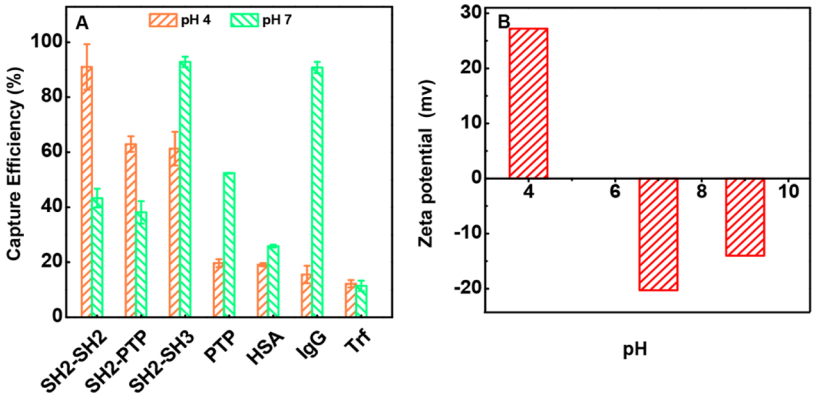

Figure 6. Adsorption selectivity and surface charge properties of the pPeps@SiO_2 microspheres. Capture efficiencies of different standard proteins on pPeps@SiO_2 microspheres at various pH values (A), Zeta potential measurements of pPeps@SiO_2 microspheres under the same pH conditions (B). Experimental conditions: protein solution, 100 mg·L^{-1}, 1.0 mL; pPeps@SiO_2 microspheres, 2 mg; adsorption time, 30 min.

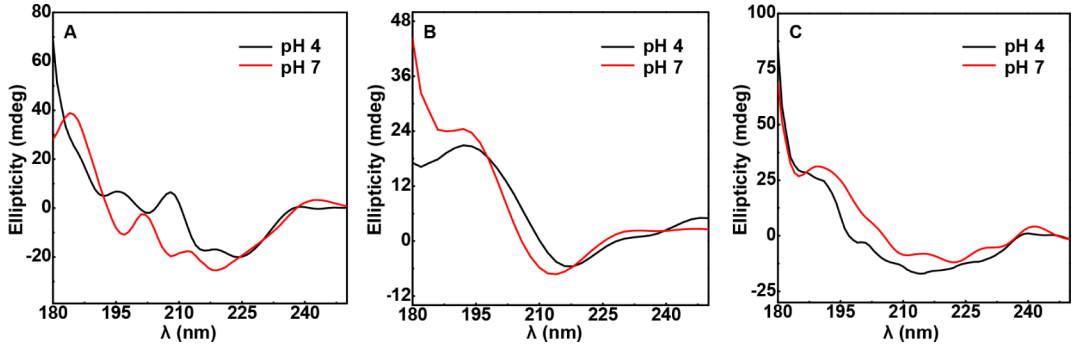

Figure 7. CD spectra of SH2−SH2 (A), SH2−SH3 (B), and SH2−PTP (C) at different pH buffers.

61.3%, and 62.96%, respectively. While at the same pH conditions, the adsorption of non-SH2 proteins is rather poor, and adsorption efficiencies for PTP, HSA, IgG, and Trf are 19.67%, 19.14%, 15.53%, and 12.18%, respectively. The adsorption difference between SH2 domain-containing proteins and non-SH2 proteins can be attributed to multivalent interactions between the SH2 motifs and the peptide chains anchored on the SiO_2 microsphere surface. It is proposed that electrostatic interactions may occur between Arg205 (βD1) in the SH2 domain and both the phosphorylated tyrosine residue and the second Glu residue near the phosphorylated tyrosine in the peptide chain of pPeps@SiO_2 microspheres. Additionally, potential hydrogen bonding might be formed between Lys200 (βD3) and/or Tyr202 (βD5) of the β-4 strand in the SH2 domain and the first Glu residue near the phosphorylated tyrosine. At the same time, the Ile in the peptide chain is likely to bind to the hydrophobic pocket of the SH2 domain through van der Waals forces, which possibly consist of the methyl groups of Tyr202 (βD5), Thr215 (EF1), and the side chains of Ile214 (βE4) and Leu237 (BG4).[25] These multiple interactions thus contribute to the favorable adsorption of SH2 domain proteins on pPeps@SiO_2 microspheres.

The capture efficiency of the material for SH2−SH3 at pH 7 is significantly higher than that of SH2−SH2 and SH2−PTP. This is because the phosphorylated tyrosine peptide chain mainly binds to specific sites in the β-sheet in the SH2 domain.[52] At pH 7, the fibrous SiO_2 microspheres display a net negative surface charge due to the deprotonation of silanol and carboxyl groups. The SH2 fusion proteins used in this study have theoretical isoelectric points between 6.5 and 7.2, indicating that at pH 7 they are close to neutral or mildly positively charged. More importantly, positively charged residues near the phosphotyrosine-binding site of SH2 domains enable favorable electrostatic interactions with the negatively charged microsphere surface, enhancing binding specificity. It can be seen from the circular dichroism spectrum that SH2−SH3 presents a configuration dominated by β-sheets (Figure 7B), which is structurally compatible with the canonical β-sheet-based phosphotyrosine-binding groove of SH2 domains. In contrast, SH2−SH2 and SH2−PTP (Figure 7A and C) exhibit mixed secondary structures rather than clear α-helix dominance, suggesting partial disruption or shielding of the β-sheet interface involved in peptide recognition. This structural variation may arise from domain−domain packing (in SH2−SH2) or interference by adjacent functional domains (e.g., the PTP domain in SH2−PTP), which could reduce the binding site accessibility. These conformational effects likely weaken the interaction between the peptide and the SH2 domain, thus reducing the capture efficiency. The sudden increase in the capture efficiency of IgG at pH 7 is due to the fact that IgG is positively charged when the pH of the solution is 7, and the pPeps@SiO_2 microspheres are negatively charged at this time (Figure 6B). There is an electrostatic force between the pPeps@SiO_2 microspheres and IgG.

Capturing of SH2 Domain Protein from Human Plasma by pPeps@SiO_2 Microspheres. As the as-prepared pPeps@SiO_2 microspheres exhibit superior adsorption performance toward SH2 domain proteins over non-SH2 proteins, their potential for selectively capturing SH2-containing proteins from human plasma was further explored. In order to highlight the capturing ability of pPeps@SiO_2 microspheres, 1 mL of a plasma sample spiked with 100 μg mL^{-1} SH2−SH3

https://doi.org/10.1021/acsomega.5c04034
ACS Omega 2025, 10, 55316−55324

protein was subjected to the adsorption procedure and then recovered with an imidazole solution (0.1 mol L^{-1}).

SDS-PAGE analysis was carried out following Laemmli's protocol, employing a conventional discontinuous buffer system.[53] As shown in Figure 8, multiple protein bands are

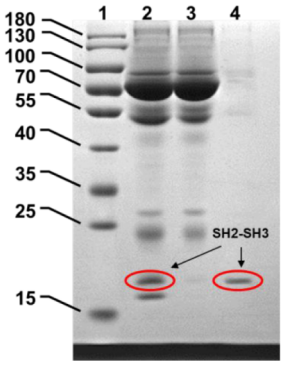

Figure 8. SDS-PAGE analysis of the SH2 domain protein enrichment from plasma using pPeps@SiO_2 microspheres. Lane 1: protein molecular weight markers (kDa); Lane 2: 100-fold diluted human plasma spiked with SH2−SH3; Lane 3: supernatant after treatment with pPeps@SiO_2 microspheres; Lane 4: protein eluate recovered after desorption.

observed in the untreated human plasma sample (Lane 2), corresponding to a wide molecular weight range of 6.5−200 kDa. These bands are primarily attributed to IgG (150 kDa), transferrin (Trf, 80 kDa), human serum albumin (HSA, 66.4 kDa), IgG heavy chain (50.0 kDa), IgG light chain (25.0 kDa), and SH2−SH3 (22.11 kDa), as well as other low-abundance proteins. Lane 3 displays the result of the supernatant treated with pPeps@SiO_2 microspheres. It can be seen that after treatment with pPeps@SiO_2 microspheres, there is almost no change in the bands of high-abundance plasma proteins HSA, IgG, and Trf in the plasma, while the bands of SH2−SH3 are significantly lighter. Lane 4 is the recovered solution, in which only one band of SH2−SH3 appears, suggesting that pPeps@SiO_2 microspheres can efficiently capture SH2 domain proteins from plasma and eliminate the interference of high-abundance proteins.

In order to ascertain the efficiency of pPeps@SiO_2 microspheres in capturing SH2 domain proteins from plasma, the contents of SH2 domain proteins in raw plasma and plasma after capturing are quantified using a Human Csk/Src molecule C-terminal kinase (C-src) enzyme-linked immunoassay kit. As shown in Figure 9, the original concentration of SH2 domain protein detected in plasma is determined to be 12.4 pg mL^{-1}, and the final concentration of SH2 domain protein in the recovered solution is determined to be 61.59 pg mL^{-1}, indicating a total recovery of 61.59 pg of SH2 domain proteins. This corresponds to a 5.1-fold enrichment, further demonstrating the microspheres' selective capture capability from complex biological samples.

CONCLUSIONS

The SH2 domain plays a crucial role in signal transduction pathways mediated by tyrosine kinases. The abnormality of the signal transduction pathway involving the SH2 domain is related to a variety of tumors and genetic diseases. A novel phosphorylated peptide chain-functionalized pPeps@SiO_2 microsphere has been prepared. Attributed to its structural

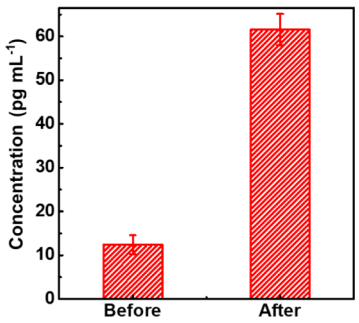

Figure 9. Quantitative enrichment of SH2 domain proteins from human plasma by pPeps@SiO_2 microspheres. The results confirm the effective capture and recovery of target SH2 proteins from complex biological samples, highlighting the practical applicability of the designed material.

features and specific interactions between phosphorylated peptide chains and SH2 domains, the pPeps@SiO_2 microspheres exhibit excellent adsorption selectivity and high binding capacity for SH2 domain-containing proteins. The pPeps@SiO_2 microsphere can eliminate the interference of high-peak proteins and effectively separate and purify proteins containing the SH2 domain from human plasma, providing effective help for further research on the relationship between SH2 domain proteins and cancer.

ASSOCIATED CONTENT

Supporting Information

The Supporting Information is available free of charge at https://pubs.acs.org/doi/10.1021/acsomega.5c04034.

Materials and reagents and Instruments. The fabrication of pPeps@SiO_2 microspheres. ESI-MS/MS of SH2 domain−peptide Complexes. Capture of SH2−SH3 proteins from plasma using pPeps@SiO_2 microspheres. Isolation and detection of SH2 domain proteins from human plasma. DTG curves of pPeps@SiO_2 microspheres. The SDS-PAGE assay results of expressed protein. The codon optimized SH−SH2 sequence for *E. coli* expression. The codon optimized SH2−SH3 sequence for *E. coli* expression. The codon optimized SH2−PTP sequence for *E. coli* expression. The codon optimized PTP sequence for *E. coli* expression (PDF)

AUTHOR INFORMATION

Corresponding Authors

Xue Hu − *School of Pharmacy, Shenyang Medical College, Shenyang 110034, China; Shenyang Key Laboratory of Medical Molecular Theranostic Probes in School of Pharmacy, Shenyang Medical College, Shenyang 110034, China;* orcid.org/0009-0002-9803-6070; Phone: +86 24 62215711; Email: huxue@symc.edu.cn; Fax: +86 24 62215711

Qing Chen − *School of Pharmacy, Shenyang Medical College, Shenyang 110034, China; Shenyang Key Laboratory of Medical Molecular Theranostic Probes in School of Pharmacy, Shenyang Medical College, Shenyang 110034, China;* orcid.org/0000-0001-6251-8292; Phone: +86 24 62215711; Email: chenqing.0906@163.com; Fax: +86 24 62215711

https://doi.org/10.1021/acsomega.5c04034
ACS Omega 2025, 10, 55316−55324

Authors

Zhen-Cun Cai − *Department of Orthopedic Surgery, The Second Affiliated Hospital of Shenyang Medical College, Shenyang 110034, China*

Long-Long Zhao − *School of Pharmacy, Shenyang Medical College, Shenyang 110034, China*

Complete contact information is available at: https://pubs.acs.org/10.1021/acsomega.5c04034

Notes

ETHICS: All human whole blood experiments were conducted in accordance with applicable laws and institutional guidelines, with approval from the ethics committee of Shenyang Medical College.

The authors declare no competing financial interest.

■ ACKNOWLEDGMENTS

This work was supported by the PhD Start-up Foundation of Liaoning Province (2022-BS-339), the Natural Science Foundation Project of Liaoning Province (No. 2024-MS-222), and the Science and Technology Foundation of Shenyang Medical College (20229049), the Key R&D Project of the Liaoning Provincial Department of Science and Technology (2025JH2/102800051), the Future Industry Frontier Technology Project of the Liaoning Provincial Department of Science and Technology (2025080219-JH2/1013).

■ REFERENCES

(1) Seet, B. T.; Dikic, I.; Zhou, M. M.; Pawson, T. Reading protein modifications with interaction domains. *Nat. Rev. Mol. Cell Biol.* **2006**, *7*, 473−483.

(2) Sadowski, I.; Stone, J. C.; Pawson, T. A noncatalytic domain conserved among cytoplasmic protein-tyrosine kinases modifies the kinase function and transforming activity of Fujinami sarcoma virus P130 gag-fps. *Mol. Cell Biol.* **1986**, *6*, 4396−4408.

(3) Liu, B. A.; Shah, E.; Jablonowski, K.; Stergachis, A.; Engelmann, B.; Nash, P. D. The SH2 Domain−Containing Proteins in 21 Species Establish the Provenance and Scope of Phosphotyrosine Signaling in Eukaryotes. *Sci. Signal.* **2011**, *4* (202), ra83.

(4) Kaneko, T.; Huang, H.; Zhao, B.; Li, L.; Liu, H.; Voss, C. K.; Wu, C.; Schiller, M. R.; Li, S. S.-C. Loops govern SH2 domain specificity by controlling access to binding pockets. *Sci. Signal.* **2010**, *3* (120), ra34.

(5) Waksman, G.; Kumaran, S.; Lubman, O. SH2 domains: Role, structure and implications for molecular medicine. *Expert Rev. Mol. Med.* **2004**, *6*, 1−18.

(6) Booker, G. W.; Breeze, A. L.; Downing, A. K.; Panayotou, G.; Gout, I.; Waterfield, M. D.; Campbell, I. D. Structure of an SH2 domain of the p85 α subunit of phosphatidylinositol-3-OH kinase. *Nature* **1992**, *358*, 684−687.

(7) Overduin, M.; Rios, C. B.; Mayer, B. J.; Baltimore, D.; Cowburn, D. Three-dimensional solution structure of the src homology 2 domain of c-abl. *Cell* **1992**, *70*, 697−704.

(8) Waksman, G.; Kominos, D.; Robertson, S. C.; Pant, N.; Baltimore, D.; Birge, R. B.; Cowburn, D.; Hanafusa, H.; Mayer, B. J.; Overduin, M.; Resh, M. D.; Rios, C. B.; Silverman, L.; Kuriyan, J. Crystal structure of the phosphotyrosine recognition domain SH2 of v-src complexed with tyrosine-phosphorylated peptides. *Nature* **1992**, *358*, 646−653.

(9) Eck, M. J.; Shoelson, S. E.; Harrison, S. C. Recognition of a high-affinity phosphotyrosyl peptide by the Src homology-2 domain of p56lck. *Nature* **1993**, *362*, 87−91.

(10) Anderson, D.; Koch, C. A.; Grey, L.; Ellis, C.; Moran, M. F.; Pawson, T. Binding of SH2 domains of phospholipase C gamma 1, GAP, and Src to activated growth factor receptors. *Science* **1990**, *250*, 979−982.

(11) Koch, C. A.; Anderson, D.; Moran, M. F.; Ellis, C.; Pawson, T. SH2 and SH3 domains: Elements that control interactions of cytoplasmic signaling proteins. *Science* **1991**, *252*, 668−674.

(12) Moran, M. F.; Koch, C. A.; Anderson, D.; Ellis, C.; England, L.; Martin, G. S.; Pawson, T. Src homology region 2 domains direct protein-protein interactions in signal transduction. *Proc. Natl. Acad. Sci. U. S. A.* **1990**, *87*, 8622−8626.

(13) Matsuda, M.; Mayer, B. J.; Fukui, Y.; Hanafusa, H. Binding of transforming protein, P47gag-crk, to a broad range of phosphotyrosine-containing proteins. *Science* **1990**, *248*, 1537−1539.

(14) Mayer, B. J.; Jackson, P. K.; Baltimore, D. The noncatalytic src homology region 2 segments of abl tyrosine kinase binds to tyrosine-phosphorylated cellular proteins with high affinity. *Proc. Natl. Acad. Sci. U. S. A.* **1991**, *88*, 627−631.

(15) Avizienyte, E.; Fincham, V. J.; Brunton, V. G.; Frame, M. C. Src SH3/2 domain-mediated peripheral accumulation of Src and phospho-myosin is linked to deregulation of e-cadherin and the epithelial-mesenchymal transition. *Mol. Biol. Cell* **2004**, *15* (6), 2794−2803.

(16) Young, M. A.; Gonfloni, S.; Superti-Furga, G.; Roux, B.; Kuriyan, J. Dynamic coupling between the SH2 and SH3 domains of c-Src and Hck underlies their inactivation by C-terminal tyrosine phosphorylation. *Cell* **2001**, *105* (1), 115−126.

(17) Roche-Lestienne, C.; Soenen-Cornu, V.; Grardel-Duflos, N.; Lai, J. L.; Philippe, N.; Facon, T.; Fenaux, P.; Preudhomme, C. Several types of mutations of the Abl gene can be found in chronic myeloid leukemia patients resistant to STI571, and they can pre-exist to the onset of treatment. *Blood* **2002**, *100* (3), 1014−1018.

(18) Liu, W.-Q.; Vidal, M.; Olszowy, C.; Million, E.; Lenoir, C.; Dhotel, H.; Garbay, C. Structure-activity relationships of small phosphopeptides, inhibitors of Grb2 SH2 domain, and their prodrugs. *J. Med. Chem.* **2004**, *47*, 1223−1233.

(19) Nagy, N.; Takahara, M.; Nishikawa, J.; Bourdon, J. C.; Kis, L. L.; Klein, G.; Klein, E. Wild-type p53 activates SAP expression in lymphoid cells. *Oncogene* **2004**, *23*, 8563−8570.

(20) Vetrie, D.; Vorechovsky, I.; Sideras, P.; Holland, J.; Davies, A.; Flinter, F.; Hammarstrom, L.; Kinnon, C.; Levinsky, R.; Bobrow, M.; Smith, C. I. E.; Bentley, D. R. The gene involved in X-linked agammaglobulinaemia is a member of the src family of protein-tyrosine kinases. *Nature* **1993**, *361*, 226−233.

(21) Brdicka, T.; Kadlecek, T. A.; Roose, J. P.; Pastuszak, A. W.; Weiss, A. Intramolecular regulatory switch in ZAP-70: Analogy with receptor tyrosine kinases. *Mol. Cell. Biol.* **2005**, *25*, 4924−4933.

(22) Tartaglia, M.; Niemeyer, C. M.; Fragale, A.; Song, X. L.; Buechner, J.; Jung, A.; Hahlen, K.; Hasle, H.; Licht, J. D.; Gelb, B. D. Somatic mutations in PTPN11 in juvenile myelomonocytic leukemia, myelodysplastic syndromes and acute myeloid leukemia. *Nat. Genet.* **2003**, *34*, 148−150.

(23) Kofoed, E. M.; Hwa, V.; Little, B.; Woods, K. A.; Buckway, C. K.; Tsubaki, J.; Pratt, K. L.; Bezrodnik, L.; Jasper, H.; Tepper, A.; Heinrich, J. J.; Rosenfeld, R. G. Growth hormone insensitivity associated with a STAT5b mutation. *N. Engl. J. Med.* **2003**, *349*, 1139−1147.

(24) Avizienyte, E.; Fincham, V. J.; Brunton, V. G.; Frame, M. C. Src SH3/2 domain-mediated peripheral accumulation of Src and phospho-myosin is linked to deregulation of e-cadherin and the epithelial-mesenchymal transition. *Mol. Biol. Cell* **2004**, *15* (6), 2794−2803.

(25) Zhou, S.; Shoelson, S. E.; Chaudhuri, M.; Gish, G.; Pawson, T.; Haser, W. G.; King, F.; Roberts, T.; Ratnofsky, S.; Lechleider, R. J.; Neel, B. G.; Birge, R. B.; Fajardo, J. E.; Chou, M. M.; Hanafusa, H.; Schaffhausen, B.; Cantley, L. C. SH2 domains recognize specific phosphopeptide sequences. *Cell* **1993**, *72*, 767−778.

(26) Fantl, W. J.; Escobedo, J. A.; Martin, G. A.; Turck, C. W.; Del Rosario, M.; McCormick, F.; Williams, L. T. Distinct phosphotyrosines on a growth factor receptor bind to specific molecules that mediate different signaling pathways. *Cell* **1992**, *69*, 413−423.

(27) Reth, M. Antigen receptor tail clue. *Nature* **1989**, *338*, 383−384.
(28) Chan, A. C.; Iwashima, M.; Turck, C. W.; Weiss, A. ZAP-70; A 70 kd protein-tyrosine kinase that associates with the TCR ζ chain. *Cell* **1992**, *71*, 649−662.
(29) Testini, C.SH2-Domain Protein Isolation Using Synthetic Phosphorylated Peptides to Study VEGFR2 Signaling*VEGF Signaling: Methods and Protocols*Methods in Molecular Biology-Springer2022247597−111
(30) Höfener, M.; Heinzlmeir, S.; Kuster, B.; Sewald, N. Probing SH2-domains using Inhibitor Affinity Purification (IAP). *Proteome Sci.* **2014**, *12*, 41.
(31) Schneider, D.; Mehlhorn, D.; Zeigermann, P.; Karger, J.; Valiullin, R. Transport properties of hierarchical micro-mesoporous materials. *Chem. Soc. Rev.* **2016**, *45*, 3439−3467.
(32) Lopez-Orozco, S.; Inayat, A.; Schwab, A.; Selvam, T.; Schwieger, W. Zeolitic materials with hierarchical porous structures. *Adv. Mater.* **2011**, *23*, 2602−2615.
(33) Perez-Ramirez, J.; Christensen, C. H.; Egeblad, K.; Christensen, C. H.; Groen, J. C. Hierarchical zeolites: Enhanced utilisation of microporous crystals in catalysis by advances in materials design. *Chem. Soc. Rev.* **2008**, *37*, 2530−2542.
(34) Xie, Y.; Wang, J.; Wang, M.; Ge, X. Fabrication of fibrous amidoxime-functionalized mesoporous silica microsphere and its selectively adsorption property for Pb^{2}+ In Aqueous Solution. *J. Hazard. Mater.* **2015**, *297*, 66−73.
(35) Thankamony, A. S. L.; Lion, C.; Pourpoint, F.; Singh, B.; Linde, A. J. P.; Carnevale, D.; Bodenhausen, G.; Vezin, H.; Lafon, O.; Polshettiwar, V. Insights into the catalytic activity of nitridated fibrous silica (KCC-1) nanocatalysts from ^{15}N and ^{29}Si NMR spectroscopy enhanced by dynamic nuclear polarization. *Angew. Chem., Int. Ed.* **2015**, *54*, 2190−2193.
(36) Fihri, A.; Cha, D.; Bouhrara, M.; Almana, N.; Polshettiwar, V. Fibrous Nano-Silica (KCC-1)-Supported Palladium Catalyst: Suzuki Coupling Reactions Under Sustainable Conditions. *ChemSuschem* **2012**, *5*, 85−89.
(37) Cate, D. M.; Adkins, J. A.; Mettakoonpitak, J.; Henry, C. S. Recent Developments in Paper-Based Microfluidic Devices. *Anal. Chem.* **2015**, *87*, 19−41.
(38) Zhang, H.; Li, Z.; Xu, P.; Wu, R.; Jiao, Z. A facile two-step synthesis of novel chrysanthemum-like mesoporous silicananoparticles for controlled pyrene release. *Chem. Commun.* **2010**, *46*, 6783−6785.
(39) Visser, A. E.; Swatloski, R. P.; Reichert, W. M.; Mayton, R.; Sheff, S.; Wierzbicki, A.; Davis, J. H., Jr.; Rogers, R. D. Task-specific ionic liquids for the extraction of metal ions from aqueous solutions. *Chem. Commun.* **2001**, 135−136.
(40) Songyang, Z.; Shoelson, S. E.; Chaudhuri, M.; Gish, G.; Pawson, T.; Haser, W. G.; King, F.; Roberts, T.; Ratnofsky, S.; Lechleider, R. J.; et al. SH2 domains recognize specific phosphopeptide sequences. *Cell* **1993**, *72* (5), 767−778.
(41) Liu, B. A.; Engelmann, B. W.; Nash, P. D. High-throughput analysis of phosphotyrosine recognition domains. *Protein Sci.* **2006**, *15* (5), 1215−1228.
(42) Frank, D. A.; Kutok, J. L.; Liang, M. C.; Schlaepfer, D. D. STAT3 participates in the development of transformation induced by v-Src. *Mol. Cell. Biol.* **1997**, *17* (11), 6149−6157.
(43) Goldstein, J. I.; Newbury, D. E.; Michael, J. R.; Ritchie, N. W.; Scott, J. H. J.; Joy, D. C. *Scanning Electron Microscopy and X-ray Microanalysis*, 4th ed.; Springer: New York, 2017.
(44) Lu, Y.; Yin, Y.; Mayers, B. T.; Xia, Y. Modifying the Surface Properties of Superparamagnetic Iron Oxide Nanoparticles through a Sol-Gel Approach. *Nano Lett.* **2002**, *2* (3), 183−186.
(45) Kango, S.; Kalia, S.; Celli, A.; Njuguna, J.; Habibi, Y.; Kumar, R. Surface Modification of Inorganic Nanoparticles for Development of Organic-Inorganic Nanocomposites: A Review. *Prog. Polym. Sci.* **2013**, *38* (8), 1232−1261.
(46) Li, H.; Cao, C.; Liu, J.; Shi, Y.; Si, R.; Gu, L.; Song, W. Cobalt single atoms anchored on N-doped ultrathin carbon nanosheets for selective transfer hydrogenation of nitroarenes. *Sci. China Mater.* **2019**, *62*, 1306−1314.
(47) Du, X.; Wang, Y.; Qu, F.; Li, K.; Liu, X.; Wang, Z.; Li, G.; Liang, H. Impact of bubbly flow in feed channel of forward osmosis for wastewater treatment: Flux performance and biofouling. *Chem. Eng. J.* **2017**, *316*, 1047−1058.
(48) Zubarev, R. A.; Makarov, A. Orbitrap Mass Spectrometry. *Anal. Chem.* **2013**, *85* (11), 5288−5296.
(49) Fenn, J. B.; Mann, M.; Meng, C. K.; Wong, S. F.; Whitehouse, C. M. Electrospray Ionization for Mass Spectrometry of Large Biomolecules. *Science* **1989**, *246* (4926), 64−71.
(50) Kaltashov, I. A.; Mohimen, A. Estimates of Protein Surface Areas in Solution by Electrospray Ionization Mass Spectrometry. *Anal. Chem.* **2005**, *77* (16), 5370−5379.
(51) Loo, J. A. Studying Noncovalent Protein Complexes by Electrospray Ionization Mass Spectrometry. *Mass Spectrom. Rev.* **1997**, *16* (1), 1−23.
(52) Yaffe, M. B. Phosphotyrosine-binding domains in signal transduction. *Nat. Rev. Mol. Cell Biol.* **2002**, *3*, 177−186.
(53) Elkak, A.; Ismail, S.; Uzun, L.; Denizli, A. Adsorption study of immunoglobulin G subclasses from different species by pseudobioaffinity separation on histidyl-bisoxirane-sepharose. *Chromatographia* **2009**, *69*, 1161−1167.

https://doi.org/10.1021/acsomega.5c04034
ACS Omega 2025, 10, 55316−55324